Ecosystems (2021) 24: 284–300
https://doi.org/10.1007/s10021-020-00518-3

ECOSYSTEMS

Alternative Biogeochemical States of River Pools Mediated by Hippo Use and Flow Variability

Christopher L. Dutton,[1]* Amanda L. Subalusky,[1,2] Stephen K. Hamilton,[3,5] Ella C. Bayer,[1] Laban Njoroge,[4] Emma J. Rosi,[5] and David M. Post[1]

[1]*Department of Ecology and Evolutionary Biology, Yale University, 165 Prospect St, New Haven, Connecticut 06511, USA;* [2]*Department of Biology, University of Florida, Gainesville, Florida, USA;* [3]*W. K. Kellogg Biological Station and Department of Integrative Biology, Michigan State University, Hickory Corners, Michigan, USA;* [4]*National Museums of Kenya, Nairobi, Kenya;* [5]*Cary Institute of Ecosystem Studies, Millbrook, New York, USA*

Abstract

Hippopotami (hippos) are ecosystem engineers that subsidize aquatic ecosystems through the transfer of organic matter and nutrients from their terrestrial grazing, with potentially profound effects on aquatic biogeochemistry. We examined the influence of hippo subsidies on biogeochemical cycling in pools of varying hydrology and intensity of hippo use in the Mara River of Kenya. We sampled upstream, downstream, and at the surface and bottom of pools of varying volume, discharge, and hippo numbers, both before and after flushing flows. The product of hippo number and water residence time served as an index of the influence of hippo subsidies (hippo subsidy index, HSI) on aquatic biogeochemistry. Low-HSI hippo pools remained oxic between flushing flows and could be a source or sink for nutrients. High-HSI hippo pools quickly became anoxic between flushing flows and exported nutrients and byproducts of anaerobic microbial metabolism, including high concentrations of total ammonia nitrogen, hydrogen sulfide, and methane. Medium-HSI hippo pools were more similar to high-HSI hippo pools but with lower concentrations of reduced substances. Episodic high discharge events flushed pools and reset them to the oxic state. Transitions from oxic to anoxic states depended on water residence time, with faster transitions to anoxia in pools experiencing smaller flushing flows. Frequent shifts between these alternative oxic and anoxic states create heterogeneity in space and time in pools as well as in downstream receiving waters. In river systems where the influence of hippos on water quality is a concern, maintaining the natural flow regime, including flushing flows, ameliorates impacts of hippos.

Key words: Tropical river; Hippopotamus; Subsidy; Oxygen; Alternative state; Anoxia; Hypoxia; Pool; Residence time; Flow variability.

Highlights

- Hippo pools exist in alternative states—oxic or anoxic.
- Transitions to anoxic states occur quickly under high hippo loading and low water residence time.

Received 4 December 2019; accepted 25 May 2020;
published online 8 June 2020

Electronic supplementary material: The online version of this article (https://doi.org/10.1007/s10021-020-00518-3) contains supplementary material, which is available to authorized users.

Author Contributions CLD, ALS, SKH, EJR, and DMP conceived of or designed the study; CLD, ALS, SKH, ECJ, LN, EJR, and DMP Performed the research; CLD and SKH analyzed the data; and CLD, ALS, SKH, ECJ, LN, EJR, and DMP wrote the paper.

**Corresponding author; e-mail:* cldutton@gmail.com

- The biogeochemical conditions of pools are predicted by discharge, volume, and hippo number.

Introduction

Animals can alter the biogeochemical cycling and functioning of ecosystems (Naiman 1988; Hooper and others 2005; Mermillod-Blondin and Rosenberg 2006; Ehrenfeld 2010; Schmitz and others 2018). In aquatic ecosystems, these effects typically occur through feeding, excretion and egestion of organic matter and nutrients, or bioturbation of sediments, and are exacerbated where animals congregate in high densities (Kitchell and others 1979; Vanni 2002; Atkinson and others 2016; Subalusky and Post 2018). Inputs of organic matter by congregations of large animals that feed elsewhere represent resource subsidies that can influence nutrient availability, primary production, and ecosystem function (Subalusky and others 2018; Subalusky and Post 2018). Under certain conditions, decomposition of organic matter can shift systems from an oxic to an anoxic state (Groffman and others 2006; Sirota and others 2013), with implications for ecological structure and function and the cycling of biogeochemically important elements including carbon, nitrogen, phosphorus, iron, and sulfur (Rabalais 2002; Conley and others 2009; Jäntti and Hietanen 2012; Testa and Kemp 2012; Friedrich and others 2014; Dutton and others 2018).

Hippopotami (*Hippopotamus amphibius*, hippos) are large, semi-aquatic animals that exert strong influences on terrestrial (Kanga and others 2013; McCauley and others 2018) and aquatic ecosystem structure and function (Masese and others 2015; Dutton and others 2018; Stears and others 2018; Subalusky and others 2018). Hippos transport large amounts of organic matter and nutrients from terrestrial grazing lands into aquatic ecosystems where they wallow during the day (Subalusky and others 2015). Excretion and egestion by hippos can subsidize aquatic food webs (Masese and others 2015; McCauley and others 2015), but excessive loading can strongly alter community composition and ecosystem processes (Dawson and others 2016; Dutton and others 2018; Stears and others 2018).

The distribution and abundance of hippos has been greatly reduced throughout tropical and subtropical Africa (Lewison and others 2008), but in protected areas hippos can be found in very high densities, particularly when available waterbodies are scarce (Stommel and others 2016), such as during extended dry seasons. As more hippos congregate in small water bodies, their inputs of organic matter and nutrients become correspondingly larger. With sufficiently high organic matter loading, hippo pools can change from predominantly aerobic to anaerobic conditions (Wolanski and Gereta 1999; Sirota and others 2013; Stears and others 2018), which has the ability to enhance greenhouse gas emissions due to the production of large amounts of methane (Naqvi and others 2010; Holgerson and Raymond 2016). The biogeochemistry of hippo pools in relation to hippo numbers and water residence time has not yet been explored, although evidence suggests that hippo pools may exist in alternative biogeochemical states depending upon the amount of loading and degree of flushing by elevated flows from seasonal rains (Wolanski and Gereta 1999; Dutton and others 2018; Stears and others 2018).

Here we examine the relationship between hippos and biogeochemical cycling in pools of the Mara River system in Kenya (Figure 1A). Over 4000 hippos load an estimated 8563 kg (dry mass) of organic matter directly into the Kenyan reaches of the Mara River every day (Subalusky and others 2015). This organic matter loading is distributed among over 170 pools, with each pool containing from 1 to more than 100 hippos (Kanga and others 2011). The deposition and remobilization of organic matter and nutrients through the flushing of hippo pools during high discharge events have been linked to hypoxic flood pulses that alter biogeochemistry of the Mara River and sometimes cause fish kills extending up to several kilometers downriver of pools (Dutton and others 2018).

We hypothesized that pools with high numbers of hippos and long water residence times will be characterized by predominantly anaerobic microbial processes and the accumulation of reduced substances and methane in between flushing flows. We further hypothesized that episodic flushing drives state changes (Figure 1B). To test these hypotheses, we conducted a survey of aquatic biogeochemistry upstream and downstream of hippo pools, and at the surface and the bottom of each pool. We sampled pools that span a wide range of hippo numbers and water residence times and evaluated their biogeochemical characteristics in relation to the combined influence of these two variables. We also studied anoxic–oxic transitions by sampling hippo pools before and after flushing flows that temporarily restored oxic conditions.

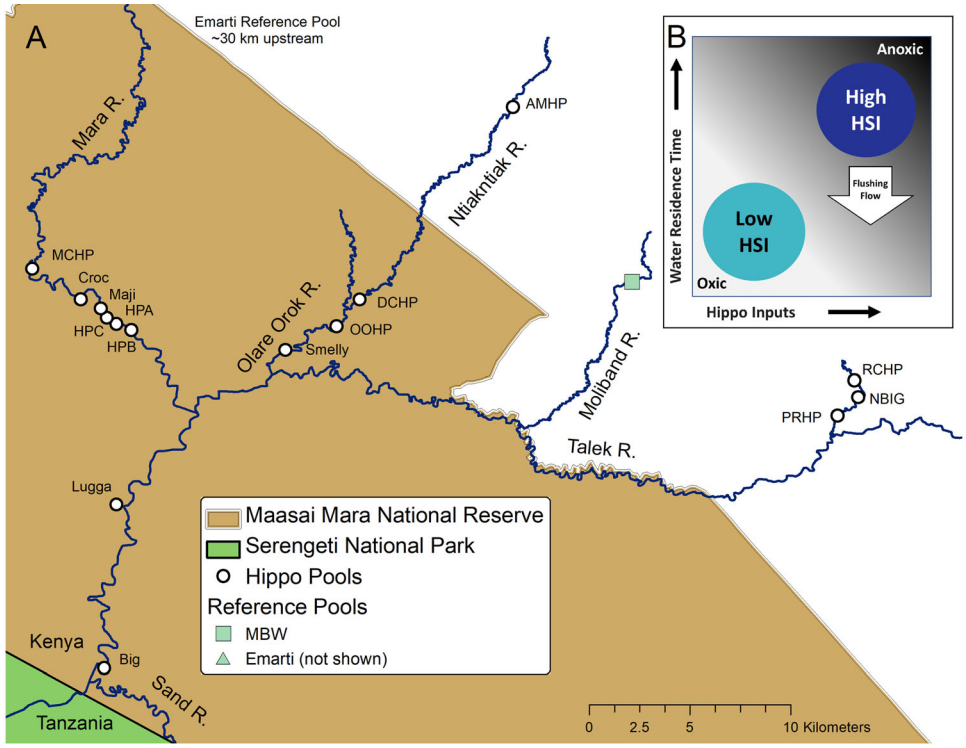

Figure 1. **A** Studied hippo pools are spread throughout the Maasai Mara National Reserve and are on the Mara, Talek, Olare Orok, Ntiakntiak, and Moliband rivers. **B** Conceptual diagram showing how hippo inputs interact with water residence time to alter biogeochemical processes within the pools, including the relative importance of aerobic or anaerobic processes. Flushing flows can temporarily change pools from anoxic to oxic states. The Hippo Subsidy Index (HSI) is the product of hippo number and water residence time.

Methods

Study Site

The Mara River of East Africa flows through the Maasai Mara National Reserve in Kenya and the upper portion of the Serengeti National Park in Tanzania (Figure 1A). The Mara River is in the upper headwaters of the Nile River and flows into Lake Victoria at Musoma, Tanzania. The Amala River and Nyangores River are the uppermost tributaries that form the Mara River near Emarti town. Several seasonal tributaries (Talek, Olare Orok, Ntiakntiak, and the Moliband) flow into the Mara River from semi-arid wildlife conservancies and domestic cattle grazing lands. Mean discharge of the Mara River at the border between Kenya and Tanzania is approximately 12 m^3 s^{-1} (range, 1–190 m^3 s^{-1}) (Subalusky and others 2018). Mean discharges of the seasonal tributaries are several orders of magnitude lower, but they are not monitored.

Hippo Pool Survey

We surveyed 17 distinct pools within the Mara River and tributaries from 2014 through 2017 (Figure 1A). We surveyed several hippo pools across multiple years, and we included two pools (Emarti and MBW) that have no recent history of use by hippos (reference pools, Figure 1A). We collected water samples at four locations from each pool (upstream, downstream, and surface and bottom water in the pool) at times when there had been no significant antecedent changes in discharge.

We were only able to locate two pools in which hippos were consistently absent (Emarti and MBW), and they are quite different from each other. Emarti is on the uppermost part of the Mara River, upstream of the wildlife conservancies. MBW is located on the Moliband River and is within one of the conservancies near Talek town that is heavily used by Maasai pastoralists. There are no hippos present in the watercourses upstream of Emarti or MBW. However, both pools are subject to potential influences of domestic livestock and other wildlife in the area. The flow regimes in the

two pools are very different; Emarti is in the main channel of the Mara River and MBW is on the Moliband, a seasonal tributary. The low sample size (only two) and distinct characteristics of the pools with no hippos make our statistical comparisons tentative. Nearly every other body of water in the area is directly affected by hippos or influenced by flow received from an upstream hippo pool.

We estimated the total number of hippos in each pool during each visit and corroborated these counts with observations of hippo abundance conducted by local Maasai as well as Conservancy rangers. River discharge was calculated downstream of each pool during each visit by measuring velocity with a handheld water flow meter (Flowatch, JDC Electronic SA, Yverdon-les-Bains, Switzerland) across a lateral transect or visually estimating approximate discharge when measurements were not possible (that is, when water depth was too low for use of a flow meter, or in the presence of aggressive hippos). We estimated pool volume by measuring the surface area of the pool in Google Earth Pro (v. 7.3) and assuming the average depth to be 1 m, the depth of water necessary to fully submerge an average hippo when resting in the pool. This assumption of pool depth was supported by field observations and surveys with a robotic boat (Dutton and others 2018). We calculated the water residence time by dividing the mean volume of water in the pool by the mean discharge. On average, the water residence time was longer in hippo pools on the tributaries than on the Mara River. Four hippo pools on the tributaries (PRHP, AMHP, DCHP and NBIG) had the highest numbers of hippos and the longest mean water residence times of all pools surveyed. AMHP and DCHP are on the Ntiakntiak River and PRHP and NBIG are on the Upper Talek River (Figure 1A).

We collected water samples from upstream and downstream of the pools using 1-liter HDPE Nalgene bottles rinsed three times with the water to be sampled. We sampled the pool surface by using approximately 20 feet of silicon tubing and a peristaltic pump (6712C Compact Portable Sampler, Teledyne ISCO Lincoln, NE, USA). The end of the tubing was attached to an empty water bottle to provide buoyancy and thrown into the center of the pool. For the bottom water sample, the weighted end of the tubing was thrown into the center of the pool and allowed to sink to the bottom. For both samples, the pump was turned on and run for several minutes prior to taking a water sample in order to rinse the tubing and, for bottom water, to ensure that sediment was not entering the sample. We measured dissolved oxygen (DO), conductivity, pH, oxidation-redox potential (ORP), temperature, turbidity, and chlorophyll-a with a Manta 2 water quality sonde (Eureka Water Probes, Austin, TX, USA) either in situ or in a thrice rinsed calibration cup immediately after taking the water sample, taking care to avoid aeration.

We took subsamples for the analysis of inorganic nutrients (NH_3 + NH_4^+, SRP, NO_3^-), dissolved organic carbon (DOC), total nitrogen (TN), total phosphorus (TP), dissolved gases (CO_2, CH_4, N_2O), hydrogen sulfide (H_2S), ferrous iron (Fe(II)), major ions (K^+, Na^+, Mg^{2+},Ca^{2+}, F^-, Cl^-, Br^-, SO_4^{2-}), and biochemical oxygen demand (BOD5). Prior to subsampling with syringes, the sample bottle was gently inverted to mix it without oxygenating the sample. All syringes and bottles were rinsed three times with the sample water prior to collection. Nalgene HDPE bottles were used to store all subsamples except for samples for H_2S and Fe(II), which were immediately added to reagents and analyzed in the field.

Hippo Pool Transitions

For a subset of the hippo pools with the highest numbers of hippos and longest average water residence times (denoted as PRHP, NBIG, DCHP, and AMHP in Figure 1), we took samples immediately after a significant increase in discharge when it appeared that the organic matter on the bottom of the pool was at least partially flushed downstream by the elevated flows. We then continued taking water samples every 2–7 days to document the changes in biogeochemistry as the elevated flows receded. We continued sampling for approximately 2 weeks, until the next flushing flow occurred. Samples were taken from the same four locations (upstream, downstream, surface, and bottom) at each time point.

We installed optical dissolved oxygen (DO) loggers (MiniDOT, PME, Inc, Vista, CA, USA) and pressure transducers (RuggedTroll 100, In Situ Inc., Fort Collins, CO, USA) in and around these hippo pools immediately after a flushing event. We installed the automated loggers at AMHP and DCHP from 10 August until 9 September 2017. Additional flushing events occurred on 22, 24, and 31 August and 1 September 2017. We installed the automated loggers at PRHP from 9 August through 8 September and at NBIG from 8 August through 24 September 2017. Additional flushing events in those pools occurred on 24 and 30 August, and 1, 6, 12, 15, 17, and 18 September 2017. In the PRHP, DCHP and AMHP pools, a DO logger was installed near the bottom in a deep section of the pool and in the river immediately

downstream of the pool. Downstream loggers were positioned in the outflow channel immediately downstream of each pool. In the NBIG hippo pool, DO loggers were installed near the surface as well as near the bottom and downstream of the pool. The pressure transducers were installed directly next to the DO logger downstream of each of the pools at a depth of approximately 0.3 meters. Each logger (DO and pressure transducer) was programmed to log data every 5 min. After retrieval, water level data were corrected if the pressure transducer had moved from the initial installation location during flushing events.

Chemical Analyses

We collected samples for dissolved inorganic nitrogen and phosphorus by filtering through a Supor 0.2-µm polyethersulfone membrane filter (Pall Corporation, Port Washington, NY, USA) directly into a collection bottle and then freezing. Once all samples were collected, the samples were thawed to ambient temperature and analyzed on a portable flow injection analyzer in the field. We analyzed total ammonia nitrogen ($NH_3 + NH_4^+$, hereafter referred to as NH_4^+) using the gas exchange method (APHA 2006), nitrate using the zinc reduction method (Ellis and others 2011), and soluble reactive phosphate (SRP) using the molybdate blue method (Murphy and Riley 1962).

We collected samples for the analysis of dissolved ferrous iron (Fe(II)) by immediately filtering the sample through a 0.2 µm Supor membrane syringe filter into a solution of 50 mM 4-(2-hydroxyethyl)-1-piperazineethanesulfonic acid buffer containing ferrozine (1 g L^{-1}) and then measuring it on a field spectrophotometer (DR 1900 Portable Spectrophotometer, Hach Company, Loveland, Colorado) (Stookey 1970; Lovley and Phillips 1987).

We measured dissolved hydrogen sulfide (H_2S) in water samples by filtering through a 0.45 µm Whatman GF/F glass fiber syringe filter (GE Healthcare Bio-Sciences, Pittsburgh, PA, USA) into glass scintillation vials and then preserving and analyzing the samples using the methylene blue method with a field spectrophotometer on the day of collection (Golterman and Clymo 1969).

We measured dissolved organic carbon (DOC) by filtering the sample water through a pre-combusted 0.45 µm Whatman GF/F glass fiber syringe filter. We preserved the sample by adding sulfuric acid to bring the pH to less than 2. Analysis took place in the USA on a Shimadzu high-temperature, platinum-catalyzed total organic carbon analyzer (Shimadzu, Kyoto, Japan).

Table 1. R^2 and p Values for Regressions of Each Biogeochemical Variable on Each Potential Explanatory Variable

Variable	HSI		Water residence time		Discharge		Hippo number	
	R^2	p value	R^2	p value	R^2	p value	R^2	p value
TP	**0.82**	*0.00*	0.64	*0.00*	0.51	*0.00*	0.00	0.94
BOD5	**0.81**	*0.00*	0.58	*0.00*	0.39	*0.02*	0.01	0.77
NH_4^+	**0.81**	*0.00*	0.51	*0.00*	0.37	*0.02*	0.00	0.84
TN	**0.78**	*0.00*	0.55	*0.00*	0.48	*0.01*	0.00	0.98
DOC	**0.76**	*0.00*	0.62	*0.00*	0.41	*0.01*	0.00	0.86
K	**0.72**	*0.00*	0.46	*0.01*	0.65	*0.00*	0.00	0.81
CH_4	**0.69**	*0.00*	0.64	*0.00*	0.33	*0.03*	0.00	0.86
CO_2	**0.60**	*0.00*	0.55	*0.00*	0.32	*0.04*	0.01	0.80
SRP	**0.58**	*0.00*	0.53	*0.00*	0.22	0.09	0.01	0.74
NO_3^-	0.47	*0.01*	0.21	0.10	**0.96**	*0.00*	0.08	0.31
Mg^{2+}	0.37	*0.02*	0.15	0.17	**0.86**	*0.00*	0.21	0.10
Ca^{2+}	0.27	0.05	0.12	0.23	**0.71**	*0.00*	0.08	0.33
H_2S	0.23	0.08	**0.29**	0.05	0.22	0.09	0.00	0.82
Cl^-	0.23	0.09	0.10	0.27	**0.58**	*0.00*	0.08	0.32
F^-	0.17	0.15	0.03	0.53	**0.73**	*0.00*	0.09	0.31
Fe(II)	0.08	0.33	0.09	0.30	**0.13**	0.20	0.07	0.37
Br^-	0.07	0.37	0.01	0.68	**0.35**	*0.02*	0.13	0.21
Na^+	0.06	0.40	0.01	0.71	**0.42**	*0.01*	0.14	0.19
SO_4^{2-}	0.00	0.83	0.05	0.46	**0.22**	0.09	0.15	0.18

Highest R^2 values boldfaced between the four potential explanatory variables. p values < 0.05 italicized.

Table 2. Biogeochemical Composition of Bottom Waters in Hippo Pools with Different Degrees of Hippo Subsidy, Showing Means with Standard Deviations (in Italics)

Biogeochemical variable	Hippo subsidy index groups				Best predictor
	None (*n* = 3)	Low (*n* = 6)	Medium (*n* = 4)	High (*n* = 5)	
TP (μg L^{-1})	419.6 ± 476.2^{a}	201.9 ± 81.3^{a}	1027.0 ± 311.9^{b}	2896.7 ± 962.6^{b}	HSI
BOD5 (mg L^{-1})	28.4 ± 38.4^{a}	7.0 ± 6.8^{a}	74.7 ± 72.7^{a}	507.7 ± 149.5^{b}	HSI
NH_4^+-N (μg L^{-1})	4930.6 ± 8391.8	26.7 ± 20.0^{a}	1281.6 ± 2326.2^{a}	13,861.0 ± 2775.2^{b}	HSI
TN (mg L^{-1})	7.0 ± 8.6^{a}	4.2 ± 1.7^{a}	10.8 ± 2.3^{ab}	27.1 ± 7.9^{b}	HSI
DOC (mg L^{-1})	7.4 ± 6.1^{a}	2.9 ± 1.5^{a}	19.4 ± 3.7^{b}	72.2 ± 33.6^{c}	HSI
K^+ (mg L^{-1})	17.2 ± 14.8^{ab}	6.4 ± 4.4^{a}	37.1 ± 20.9^{bc}	65.2 ± 17.2^{c}	HSI
CH_4 (μmol L^{-1})	2.2 ± 2.5^{a}	0.7 ± 0.6^{a}	79.4 ± 79.6^{b}	414.0 ± 239.0^{c}	HSI
CO_2 (μmol L^{-1})	95.3 ± 99.2^{a}	85.3 ± 14.3^{a}	561.9 ± 194.1^{b}	1964.0 ± 1331.0^{c}	HSI
SRP (μg L^{-1})	5.6 ± 5.8^{a}	16.5 ± 2.5^{a}	77.5 ± 152.3^{a}	1134.7 ± 803.1^{b}	HSI
NO_3^--N (μg L^{-1})	334.7 ± 494.2^{b}	1014.5 ± 65.2^{c}	9.3 ± 5.9^{a}	138.0 ± 118.4^{b}	Discharge
Mg^{2+} (mg L^{-1})	3.2 ± 1.1^{b}	1.2 ± 1.0^{a}	12.5 ± 3.1^{c}	10.4 ± 2.3^{c}	Discharge
Ca^{2+} (mg L^{-1})	19.4 ± 8.1^{b}	6.9 ± 4.4^{a}	88.8 ± 36.2^{c}	67.2 ± 19.9^{c}	Discharge
H_2S (μg L^{-1})	11.3 ± 6.0^{a}	19.5 ± 11.1^{a}	601.3 ± 811.0^{a}	861.6 ± 993.2^{a}	WRT
Cl^- (mg L^{-1})	13.8 ± 9.0^{a}	8.0 ± 5.8^{a}	76.7 ± 38.6^{b}	58.5 ± 28.2^{b}	Discharge
F^- (mg L^{-1})	1.5 ± 0.6^{b}	0.6 ± 0.2^{a}	3.5 ± 0.6^{c}	2.2 ± 0.2^{b}	Discharge
Fe(II) (μg L^{-1})	47.3 ± 59.3^{ab}	83.0 ± 140.0^{a}	2392.9 ± 4079.2^{b}	2110.5 ± 3622.5^{b}	Discharge
Br^- (mg L^{-1})	0.3 ± 0.4^{ab}	0.0 ± 0.1^{a}	5.0 ± 3.0^{c}	2.7 ± 3.1^{bc}	Discharge
Na^+ (mg L^{-1})	33.4 ± 7.3^{a}	15.8 ± 8.2^{a}	292.8 ± 162.9^{b}	140.0 ± 89.1^{b}	Discharge
SO_4^{2-} (mg L^{-1})	11.2 ± 12.2^{a}	7.7 ± 5.7^{a}	236.8 ± 134.3^{b}	34.1 ± 26.5^{a}	Discharge

Variables are ordered from top to bottom by as in Table 1. Letters indicate significant differences determined by pairwise t tests. Although no hippos were present in the pools classified as ''none,'' that does not preclude the possibility of other wildlife or domestic animals influencing the biogeochemistry (for example, we observed cattle presence at one ''no hippo'' pool that may have contributed to elevated total ammonia concentrations). Best predictor is identified for each biogeochemical variable.

We preserved unfiltered samples for total nitrogen (TN) and total phosphorus (TP) by adding sulfuric acid to bring the pH to less than 2. Preserved samples were analyzed for TN and TP on an Astoria-Pacific flow analyzer (Astoria-Pacific, Clackamas, Oregon, USA) in the USA using an alkaline potassium persulfate digestion (Hosomi and Sudo 1986). We filtered samples for major ions through a 0.45 μm Whatman GF/F glass fiber filter directly into a collection bottle and then analyzed the samples on a Dionex ion chromatograph system equipped with membrane suppression and conductivity detection (Dionex, Sunnyvale, California, USA).

We collected samples of dissolved CO_2 and CH_4 using a static headspace equilibration technique (Hamilton and Ostrom 2007). In short, we drew 115 mL of water into a 140-mL syringe with a stopcock. We then drew 25 mL of ambient air into the syringe. We gently shook the syringe for 5 min to equilibrate the headspace with the dissolved gases in the sample water. We then injected 15 mL of gas from the headspace into an evacuated Exetainer (Labco, Ceredigion, UK) and stored it within water-filled 50-mL Falcon tubes or a water-filled 1-liter Nalgene bottle. We analyzed preserved samples of dissolved gases on a Shimadzu GC-2014 gas chromatograph (Shimadzu, Kyoto, Japan) in the USA. Extended travel time and several flights were needed to get the samples back to the laboratory from the field. Standards prepared similarly that traveled with the samples and served as ''trip standards'' allowed us to account for minor changes in the gas samples due to pressure changes. Original dissolved gas concentrations were determined from Henry's Law, accounting for the slight proportion of total CO_2 and CH_4 that came from the headspace air.

We measured the biochemical oxygen demand in water samples (BOD5) by incubating a subsample diluted to 300 mL with a phosphate buffer and solutions containing magnesium sulfate, calcium chloride and ferric chloride (APHA 2006). We incubated samples for approximately 24 h within 300-mL air-tight glass bottles. We measured dissolved oxygen at the beginning and end of the incubation with a YSI ProODO optical dissolved oxygen sensor (YSI Incorporated, Yellow Springs, Ohio, USA) and linearly extrapolated the 24-h rate of dissolved oxygen consumption to 5 days. Extrapolation from a shorter incubation period was necessary because the very high oxygen demand

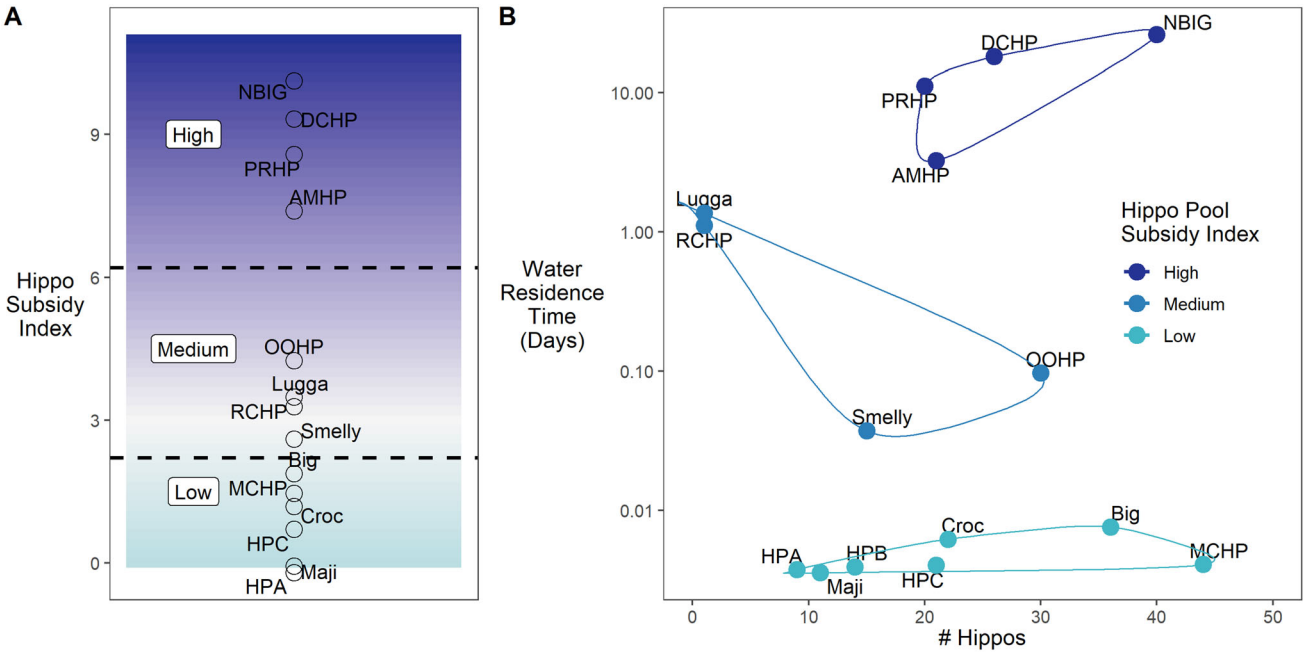

Figure 2. Hippo Subsidy Index **A** Placement of hippo pools on a gradient of Hippo Subsidy Index (HSI; here log10 transformed). Dashed lines indicate divisions between the three groups of hippo pools (high, medium, and low HSI). **B** Groupings of hippo pools roughly correspond to changes in water residence time.

often would have entirely consumed the oxygen before the end of a 5-day period; expression as BOD5 allows comparison with values for other river systems reported in the literature.

Statistical Analyses

We computed all statistical analyses in the R statistical language using $\alpha = 0.05$ to determine significance (R Core Team 2018). We provide all data and R code for the statistics in the Mendeley Data Repository (Dutton and others 2020).

To account for the influence of hippo number and water residence time (discharge/volume), we created a Hippo Subsidy Index (HSI), the product of these two variables (Figure 1 inset). We graphed hippo pools by discharge and water residence time and used the HSI index to identify natural groupings of the pools (high, medium and low). To determine whether the HSI index is a meaningful metric for understanding the biogeochemical conditions in pools, we compared linear regressions for each biogeochemical variable from the bottom water samples on each of the four potential predictors (discharge, hippo number, water residence time, and HSI).

We computed means and standard deviations for the biogeochemical variables in the bottom waters of pools by each of the three HSI groups. We determined which biogeochemical variables were significantly different among different hippo pool groups, including pools with measurements in different years without the complete set of biogeochemical variables ($N = 18$), using an ANOVA followed by Tukey's HSD post hoc test on the log-transformed values (R Core Team 2018). We confirmed that the log-transformed values from pools that grouped together had normally distributed residuals with the Shapiro–Wilk normality test ($W = 0.98$ p value = 0.96), and confirmed they had equal variance with Levene's test ($F = 0.41$, p value = 0.75).

To characterize a pool as a source or sink for riverine nutrient transport and to identify within-pool processes, we subtracted downstream values from upstream values for all measured biogeochemical variables and calculated means and standard deviations ($N = 17$; one pool did not have downstream and upstream measurements). We used the nonparametric Kruskal–Wallis and Dunn's tests to identify differences in the transformations of biogeochemical variables within the hippo pool groups on the untransformed values, which did not meet assumptions of normality or have equal variances. We used Dunn's test for nonparametric comparisons because it is not sensitive to unequal sample sizes (Zar 2010), and we

Table 3. Mean Concentration Change (Downstream Minus Upstream Values) and Standard Deviations (in Italics) for all Measured Biogeochemical Variables from Hippo Pools with Different Degrees of Hippo Subsidy

Biogeochemical variable	Hippo subsidy index groups: downstream–upstream measurements				Best predictor
	None (n = 2)	Low (n = 7)	Medium (n = 4)	High (n = 4)	
TP (μg L^{-1})	8.3 ± 3.6^{ab}	− 10.8 ± 28.0^{b}	− 37.1 ± 130.0^{ab}	2030.7 ± 1382.3^{a}	HSI
BOD5 (mg L^{-1})	10.9 ± 15.9	− 2.1 ± 7.0	− 3.5 ± 16.0	99.2 ± 390.7	HSI
NH_4^+–N (μg L^{-1})	− 29.2 ± 37.5	1047.3 ± 2665.9	43.7 ± 57.4	8598.9 ± 6028.9	HSI
TN (mg L^{-1})	0.8 ± 1.3	0.5 ± 2.0	− 0.6 ± 4.7	13.3 ± 8.8	HSI
DOC (mg L^{-1})	1.3 ± 2.3^{ab}	− 0.1 ± 0.5^{b}	2.4 ± 3.1^{ab}	49.5 ± 33.5^{a}	HSI
K^+ (mg L^{-1})	1.1 ± 2.1^{ab}	0.1 ± 0.5^{ab}	− 1.0 ± 1.8^{b}	24.6 ± 22.1^{a}	HSI
CH_4 (μmol L^{-1})	4.2 ± 6.1	0.2 ± 0.4	4.6 ± 10.3	227.4 ± 158.0	HSI
CO_2 (μmol L^{-1})	7.8 ± 2.4	1.9 ± 18.1	24.9 ± 71.8	966.6 ± 742.4	HSI
SRP (μg L^{-1})	− 7.1 ± 8.5^{ab}	− 4.5 ± 7.5^{b}	− 1120.7 ± 2249.2^{ab}	733.8 ± 780.4^{a}	HSI
NO_3^-–N (μg L^{-1})	− 91.2 ± 114.9	− 13.7 ± 37.1	0.1 ± 15.6	43.3 ± 203.3	Discharge
Mg^{2+} (mg L^{-1})	0.2 ± 0.6	0.1 ± 0.1	− 1.2 ± 1.4	1.0 ± 3.6	Discharge
Ca^{2+} (mg L^{-1})	0.8 ± 2.1	0.1 ± 0.3	− 4.2 ± 4.8	3.4 ± 29.3	Discharge
H_2S (μg L^{-1})	2.2 ± 0.4	− 2.9 ± 3.8	477.0 ± 949.7	571.9 ± 913.9	WRT
Cl^- (mg L^{-1})	0.0 ± 0.6	− 0.1 ± 0.4	− 1.2 ± 3.2	− 13.2 ± 23.3	Discharge
F^- (mg L^{-1})	0.0 ± 0.1	0.0 ± 0.0	0.0 ± 0.1	− 0.4 ± 0.4	Discharge
Fe(II) (μg L^{-1})	2.6 ± 3.7	38.7 ± 65.6	− 33.7 ± 168.5	1424.2 ± 2912.0	Discharge
Br^- (mg L^{-1})	0.0 ± 0.0	0.0 ± 0.0	− 0.3 ± 0.3	− 0.4 ± 1.8	Discharge
Na^+ (mg L^{-1})	0.2 ± 0.8	0.4 ± 0.8	− 13.6 ± 18.8	− 94.8 ± 101.2	Discharge
SO_4^{2-} (mg L^{-1})	0.0 ± 0.8^{ab}	− 0.1 ± 0.2^{b}	− 8.4 ± 10.5^{ab}	− 172.2 ± 136.2^{a}	Discharge

Variables are ordered from top to bottom as in Table 1. Letters indicate significant differences determined by the Dunn's Pairwise Comparison Test (no letter indicates no difference). Best predictor is identified for each biogeochemical variable.

present an adjusted p value using the Holm correction to account for multiple comparisons (Holm 1979).

To compare biogeochemical states before and after flushing flows of the four hippo pools with high numbers of hippos and long water residence times (that is, the highest HSIs), we computed a PCA on the log-transformed biogeochemical variables from the bottom waters of the pools before and after flushing flows using the prcomp function in R (R Core Team 2018).

Results

Hippo Pool Survey

Three groups of hippo pools were identified based on the HSI (Figure 2) that include pools spanning a wide range of hippo numbers and water residence times. High-HSI hippo pools had an average of 27 hippos (range, 20–40) and water residence times between 3 and 26 days. Medium-HSI hippo pools had an average of 12 hippos (1 to 30) and water residence time between 1 and 32 h. Low-HSI hippo pools had an average of 23 hippos (9 to 44) and water residence times between 5 and 11 min. The two reference pools with no hippos had water residence times of 3 min and 4 days, spanning much of the range of water residence times observed across the hippo pools.

The HSI was the best predictor of total N and P, NH_4^+, SRP, K^+, DOC, BOD5, and dissolved CO_2 and CH_4 (Table 1 and Figure S1). Nitrate, which was inversely related to HSI but positively related to discharge, was better predicted by discharge alone. Discharge alone was also a better predictor of the major ions Ca^{2+}, Mg^{2+}, Cl^-, and Na^+, as well as the minor ion F^-. None of the regressions for SO_4^{2-} or Fe(II) were significant, and H_2S was predicted only by water residence time, albeit not strongly. Hippo number alone was not a predictor of any of the biogeochemical variables.

The concentrations of all biogeochemical variables in the bottom waters of hippo pools varied significantly among the HSI groups (Table 2). By far the highest concentrations of BOD5, SRP, and DOC occurred in the high-HSI pools. We also found higher concentrations of Mg^{2+}, Ca^{2+}, CH_4, Na^+, CO_2, and Cl^- in high- and medium-HSI pools than in low-HSI pools and pools with no hippos. We found the highest concentrations of SO_4^{2-} in medium-HSI pools and the highest concentrations of NO_3^- in low-HSI pools. We also found higher concentrations of NH_4^+, Fe(II), H_2S, Br^-, TN, TP,

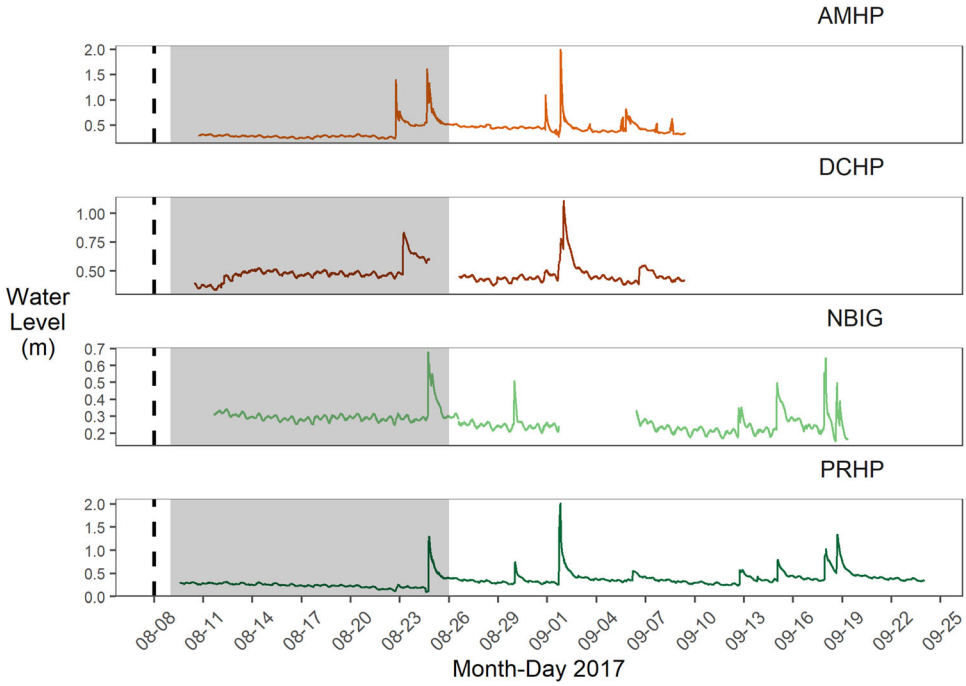

Figure 3. Water level time series for the four high-HSI hippo pools showing multiple flushing events from August 10th through September 21st, 2017. AMHP is several kilometers upstream of DCHP, and NBIG is several kilometers upstream of PRHP. Dashed line represents first known flushing event of the study period. Shaded box represents the time period of intensive biogeochemical sampling. Gaps represent missing data. Colors for pool identity correspond to those in Figures 5-6.

and K^+ in high-HSI pools compared to medium-HSI pools.

Comparisons of upstream and downstream concentrations showed that high-HSI pools had significantly higher concentrations of TP, SRP, and DOC and lower concentrations of SO_4^{2-} compared to low-HSI pools. There was a significant increase in the concentration of K^+ in high-HSI hippo pools compared to medium-HSI hippo pools. There were no significant differences in downstream vs. upstream concentrations in low-HSI hippo pools and pools with no hippos. The low sample size of pools with no hippos (N = 2) makes it difficult to distinguish them from the low-, medium- and high-HSI hippo pools.

Hippo Pool Transitions

We sampled before and after multiple flushing events in four high-HSI hippo pools (Figure 3) and found that flushing events temporarily increased the DO in surface waters in the pools for several days, after which the pools would return to anoxia (Figures 4, 5B and S2–S4). The pH remained relatively stable in the bottom waters of the pools (Figure 5C). Oxidation–reduction potential continued to fall after the flushing event and then became reset after the second flushing event (Figure 5D). Conductivity increased over time in all four pools after the flushing events (Figure 5E).

Episodic flushing by river flow events, as indicated by temporary increases in water levels, brought oxygenated water into the hippo pools, but did not always cause them to mix vertically. At AMHP, flushing events raised the water level by approximately 1 m (Figures 3 and S2) and temporarily increased the DO in the bottom of the water column (Figure S2). At DCHP, several kilometers downstream of AMHP, flushing events raised the water level by less than 1 m (Figure S3), and bottom water anoxia developed much more quickly compared to AMHP (Figures S2 and S3). NBIG hippo pool was flushed nine times over the full monitoring period (Figure 4). We recorded larger increases in surface water DO that persisted for several days before returning to anoxia, but the bottom water DO concentrations never rose, indicating that the bottom water of the pool was not likely flushed (Figure 4). The downstream DO logger recorded several large diel oxygen swings, with concentrations ranging between about 1 mg L^{-1} to more than 15 mg L^{-1}, with the high concentrations accompanied by visible algal blooms.

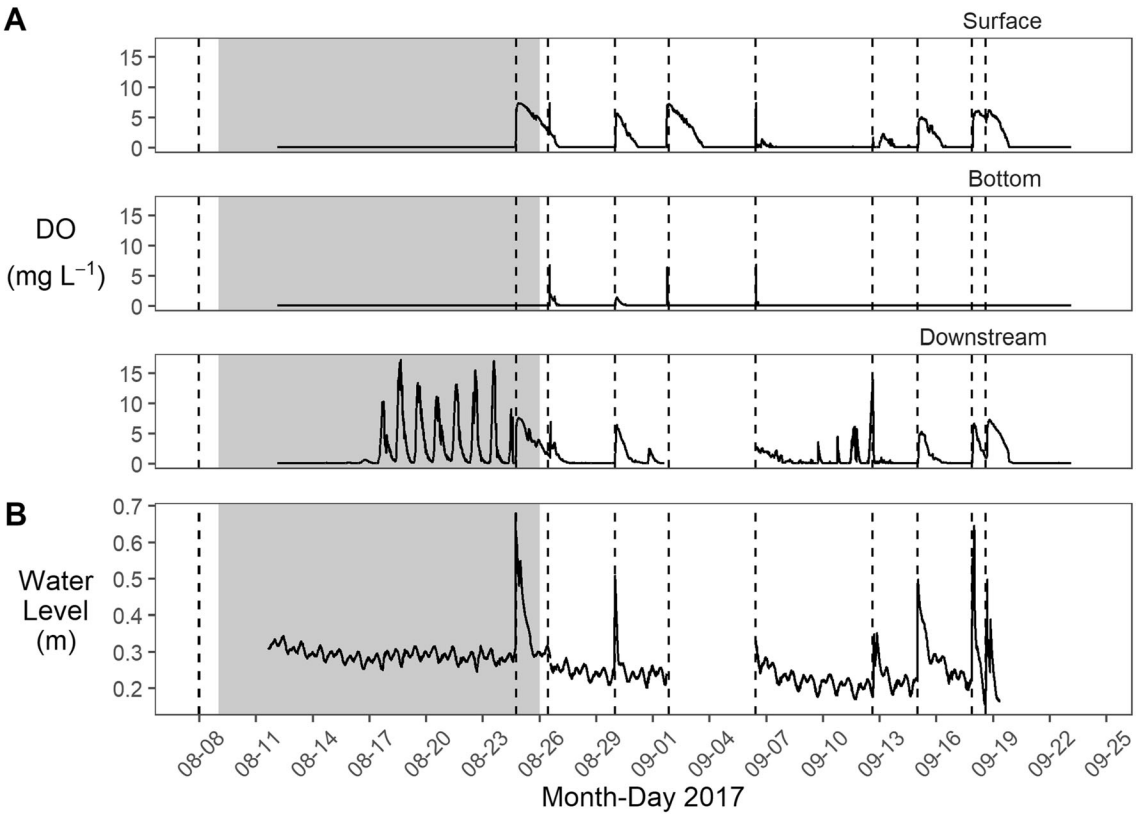

Figure 4. Dissolved oxygen (DO) and water level time series for NBIG hippo pool. **A** DO time series (5-min intervals) for water on the surface (top), bottom (middle) and immediately downstream of the pool (lower). Dashed line represents flushing events. **B** Water level (5-min intervals) time series. Shaded box represents the time period of intensive biogeochemical sampling. Loggers were installed after the first flushing event on August 7–8th, 2017.

Flushing events at PRHP, several kilometers downstream of NBIG, immediately raised the DO in the bottom water from 0 mg L^{-1}; however, it returned to anoxia within several days (Figure S4).

Concentrations of TN and NH_4^+ increased between flushing events in all four high-HSI hippo pools, with particularly large increases in PRHP (Figure 6). NO_3^- concentrations declined in all four pools between flushing events. TP and SRP concentrations rose considerably in PRHP after the first flushing event and then declined after the second flushing event (Figure 6). Concentrations of DOC and dissolved CO_2 and CH_4 increased in NBIG, with larger increases in the further downstream pool, PRHP, after the first flushing event (Figure 6). SO_4^{2-} concentrations declined in NBIG and PRHP and increased in AMHP and DCHP (Figure S5). H_2S concentrations increased in NBIG, and H_2S and Fe(II) concentrations increased in PRHP. Concentrations of Br^-, Ca^{2+}, Cl^-, K^+ and Mg^{2+} increased rapidly in PRHP (Figures S6 and S7). No discernable trends in concentration were evident for F^- and Na^+.

The four high-HSI hippo pools had large changes in biogeochemical variables, as indicated by changes in multivariate space on the PCA, in relation to the days since the last flushing flow (Figure 7). We found that BOD5, NH_4^+, and ORP strongly explained variation along the first axis (PC1, 49% of the explained variance). Na^+, Cl^-, pH, and specific conductivity strongly explained variation along the second axis (PC2, 15% of the explained variance). After flushing events, pools moved left in multivariate space toward anoxia and increased biogeochemical oxygen demand. The pools that share a tributary and flow patterns grouped closer together on the PCA (Figure 1; AMHP and DCHP are on the Ntiakntiak River and PRHP and NBIG are on the Upper Talek River). Within the pools that share a tributary, the downstream pool changed more rapidly over time, as indicated by the distance change in multivariate space, after the cessation of flow than the upstream pool, suggesting a possible cumulative effect of upstream hippo pools on the biogeochemistry of downstream hippo pools (Figure 7).

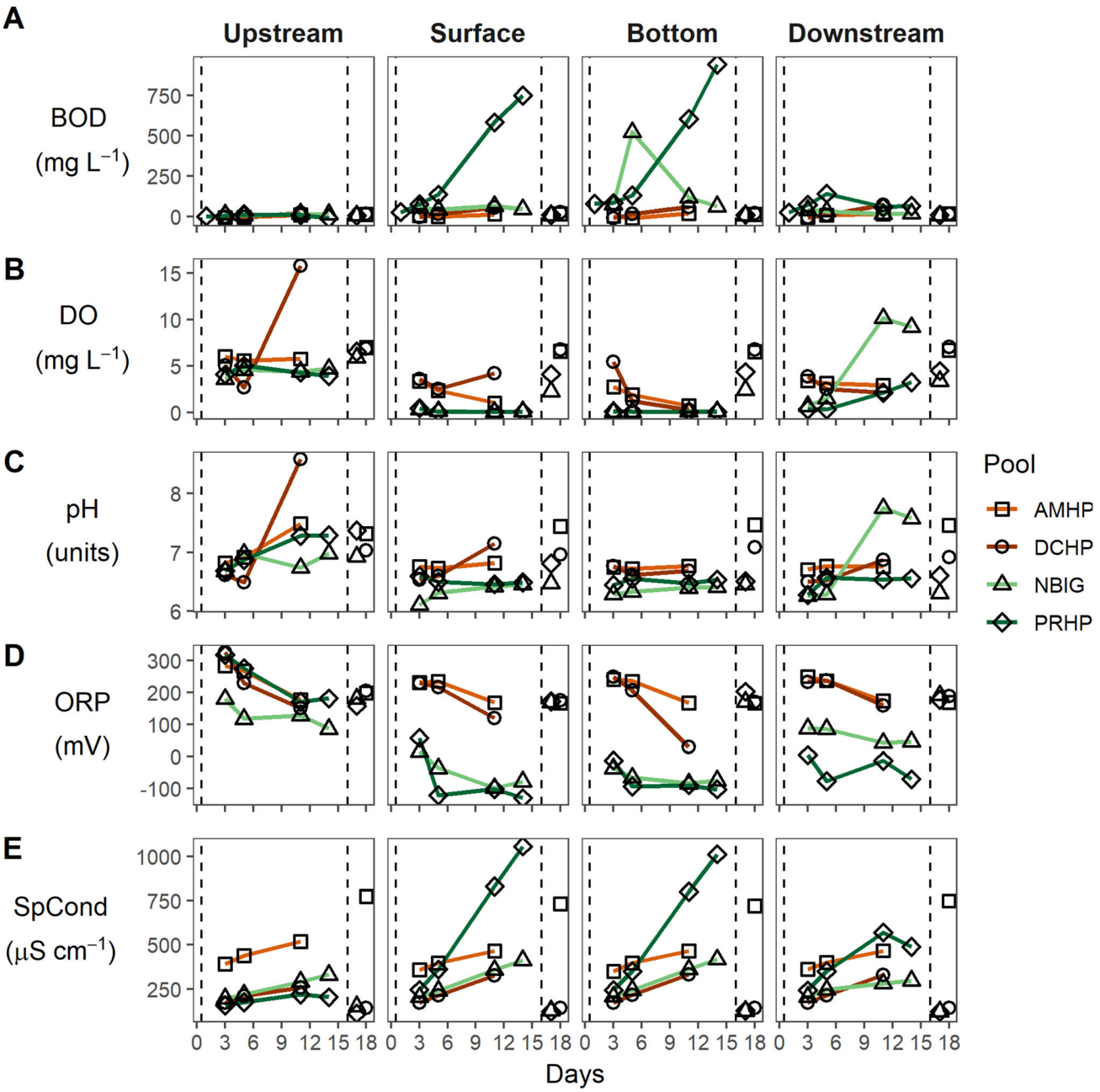

Figure 5. Upstream, surface, bottom, and downstream measurements of **A** biochemical oxygen demand (BOD), **B** dissolved oxygen (DO), **C** pH, **D** oxidation–reduction potential (ORP), and **E** specific conductivity (SpCond) for the four high-HSI hippo pools monitored every 3–6 days, starting after an initial flushing event (day 0) and continuing until a subsequent flushing event. Vertical dashed lines represent the occurrence of flushing events, and complete water level time series for each pool are shown in Figure 3.

Greenhouse Gases

We found highly elevated concentrations of dissolved free CO_2 and CH_4 in high-HSI hippo pools (Table 2). Mean CO_2 concentrations ranged from 95.3 µmol L^{-1} in pools with no hippos, to 125.9 µmol L^{-1} in low-HSI pools, 561.9 µmol L^{-1} in medium-HSI pools, and 1964 µmol L^{-1} in high-HSI pools. Mean CH_4 concentrations ranged from 2.2 µmol L^{-1} in pools with no hippos to 5 µmol L^{-1}

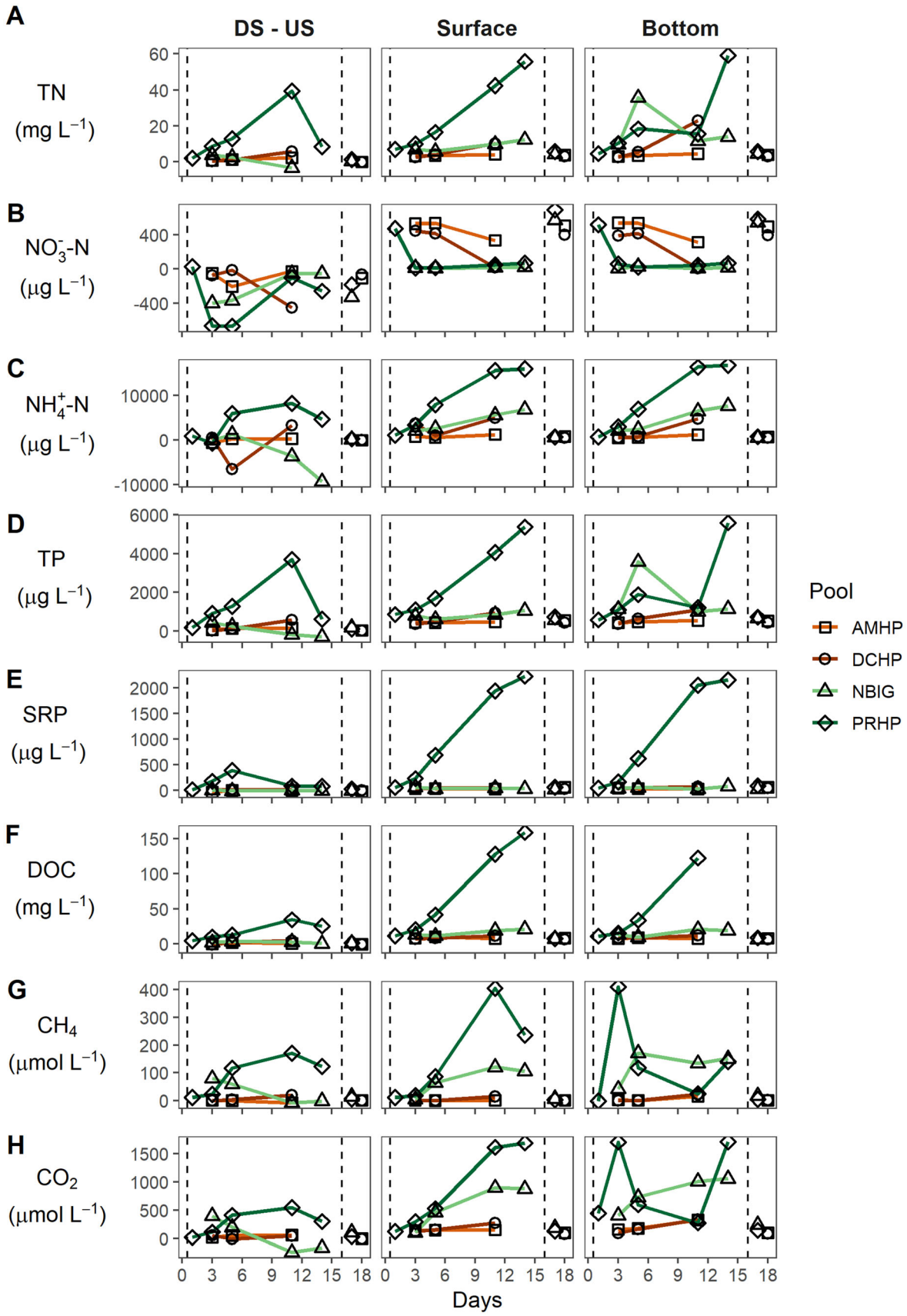
A
DS - US
Surface
Bottom
TN
(mg L−1)
B
NO3-N
(µg L−1)
C
NH4+-N
(µg L−1)
D
TP
(µg L−1)
E
SRP
(µg L−1)
F
DOC
(mg L−1)
G
CH4
(µmol L−1)
H
CO2
(µmol L−1)
Days
Pool
AMHP
DCHP
NBIG
PRHP

◀**Figure 6.** Downstream minus upstream (DS–US), surface, and bottom measurements of **A** total nitrogen (TN), **B** nitrate (NO_3^-–N), **C** ammonium (NH^{4+}–N), **D** total phosphorus (TP), **E** soluble reactive phosphorus (SRP), **F** dissolved organic carbon (DOC), **G** methane (CH_4), and **H** carbon dioxide (CO_2) for the four high-HSI hippo pools monitored every 3–6 days, starting after an initial flushing event (day 0) and continuing until a subsequent flushing event. Vertical dashed lines represent the occurrence of flushing events, and complete water level time series for each pool is in Figure 3.

in low-HSI pools, 79.4 μmol L^{-1} in medium-HSI pools, and 414 μmol L^{-1} in high-HSI pools. Concentrations of dissolved N_2O in all pools were less than 0.02 μmol L^{-1}.

Discussion

In the hippo pools of the Mara River system, the majority of the biogeochemical variables related to organic matter and nutrient subsidies were predicted better by the HSI, which considers the combined effects of hippo numbers and water residence times, than by hippo numbers, discharge, or water residence time alone (Table 1 and Figure S1). Excretion by hippos would logically affect nutrients, dissolved organic matter, and indicators of heterotrophic microbial metabolism (that is, BOD5 and dissolved CO_2 and CH_4), and the effects would be most strongly manifested in pools with long water residence times, as is evident in Table 2. Potassium would be included among the nutrients excreted at high rates because it is an abundant element in many tropical grasses (Kilham 1982). Biogeochemical variables that reflect the geology and land use of watersheds, including most major ions and NO_3^-, were better predicted by discharge alone, which is likely because the mainstem Mara River receives tributaries draining watersheds of different geology (major ions) and with significant agricultural land use (NO_3^-) compared to those with hippo pools sampled in this study (GLOWS 2007; Mwanake and others 2019).

Upstream–downstream comparisons for high-HSI pools showed significant increases in TP, SRP, DOC, and K^+, in agreement with the patterns across HSI groups, as well as decreases in SO_4^{2-} that could be due to SO^{42-} reduction in the oxygen-depleted pools (Table 3). In some medium- and high-HSI pools we observed very large changes in concentrations of NH_4^+, CO_2, H_2S, CH_4, and Fe(II), but these variables did not show statistically significant differences across groups due to high variability of pools within the groups.

Alternative States of Hippo Pools

Episodic flow events flush the pools and bring them to a common starting point reflecting the biogeochemistry of the river water, after which they diverge variably under the influence of hippo subsidies. Four pools with high HSIs that we sampled over 2 weeks following a flow event changed markedly before being reset by another event (Figures 5 and 6).

The transition from oxic to hypoxic and anoxic conditions profoundly influences the aquatic biogeochemistry and ecology within and downstream of hippo pools, and three of the four high-HSI pools we sampled passed that threshold in the 2 weeks following a flow event (Figure 5). Hippo pools thus exist in two alternative biogeochemical states characterized by the concentration of dissolved oxygen, similar to coastal marine ecosystems experiencing bouts of hypoxia (Conley and others 2009; Friedrich and others 2014). During intervals between flushing flows, bottom water and upstream–downstream differences in concentrations of biogeochemical variables in high- and medium-HSI pools reflect the predominance of anaerobic heterotrophic processes that prevail in hypoxic to anoxic conditions (Tables 2 and 3). This results in the accumulation of nutrients and dissolved CO_2 and CH_4. In contrast, the aquatic biogeochemistry of low-HSI pools and pools with no hippos do not show pronounced oxygen depletion and the resultant predominant influence of anaerobic processes.

The pool with the highest water residence time relative to hippo number, PRHP, had the quickest transition back to an anoxic state (Figure 7), along with a higher accumulation of reduced substances. This is likely due to the high hippo subsidy input rates and long water residence time in PRHP, as well as to its location several kilometers downstream of NBIG, so the water that enters PRHP from upstream is likely already influenced by hippo subsidies (Figure 1). In the high-HSI hippo pools PRHP, DCHP, and AMHP, the bottom waters became oxygenated in response to a flushing event but quickly returned to anoxia within several days (Figures S2–S4). A small weir at the downstream portion of NBIG may have prevented the complete flushing of the pool, allowing the bottom water to remain anoxic throughout the nine recorded flushing events (Figure 4).

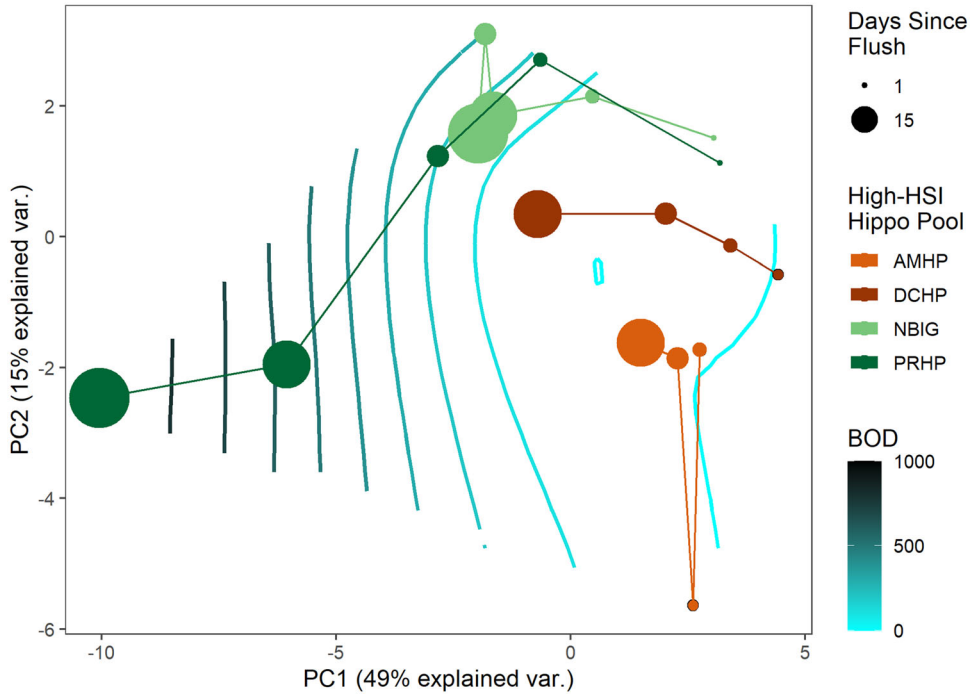

Figure 7. Principal components analysis of biogeochemical conditions in the bottom waters of the four high-HSI hippo pools (each represented as different colors) during a shift in states following cessation of a flushing flow. Pools on the same tributary are colored with the same hue, with the further downstream pool represented as a darker hue. Lines represent the BOD gradient separating the sites. Sizes of the points represent the days since the last flushing event.

Shifts between biogeochemical states within hippo pools due to periodic flushing flows may happen regularly and could be increasing in frequency with changes in climate. Increased occurrence of droughts and increasingly intense rainfalls have been documented in the Mara River Basin since the 1960s (Bartzke and others 2018). Additionally, planned water diversions from the Mara River system would likely increase the water residence time and attenuate peak flows (McClain and others 2014; Mnaya and others 2017), potentially reducing the flushing capacity of flows and shifting more hippo pools to an anoxic state. A reduction of flow in the Mara River system may increase the occurrence and duration of the anoxic state in hippo pools, likely reducing their aquatic diversity (Dawson and others 2016). The cumulative effect of the flushing of multiple hippo pools along a river channel can cause fish kills (Dutton and others 2018), and an increased frequency in the shifts between alternative biogeochemical states may alter aquatic community composition downstream.

Degradation of Water Quality

In the intervals between flow events, the water quality in high-HSI hippo pools may degrade to the point where aquatic life would be stressed. Potentially important stressors in addition to low DO include high concentrations of un-ionized ammonia (NH_{3-}), H_2S, CH_4 and/or free CO_2. High-HSI hippo pools accumulated extremely high concentrations of total ammonia nitrogen (> 13 mg N L^{-1}), exceeding levels known to impair aquatic organisms. Although most of the total ammonia nitrogen would exist as NH_4^+ at the pH of these waters, high concentrations of un-ionized NH_3 can be toxic to aquatic life (Randall and Tsui 2002), in spite of the fact that several fish endemic to the area are adapted to survive in high ammonia environments (Chew and others 2005; Loong and others 2007). The high concentrations of H_2S observed within some of the high-HSI hippo pools are also toxic to most species of fishes (Smith and others 1976). In addition, the high concentrations of CO_2 observed in high-HSI hippo pools could induce hypercapnia in aquatic organisms with gills, resulting in alterations in behavior (McNeil and Sasse 2016). Although not toxic, high concentrations of CH_4 can be harmful to aquatic organisms due to the displacement of oxygen or depletion of DO through the rapid oxidation of CH_4 (Bastviken 2009). We measured concentrations of dissolved CH_4 over 10 mg L^{-1} at one hippo pool, approaching the level that would pose an explosive

hazard should the CH_4 be released into a confined air space (Eltschlager and others 2001; Osborn and others 2011).

BOD5 within high-HSI hippo pools was in the range of values reported for untreated domestic sewage, yet orders of magnitude lower than waste lagoons of livestock operations (Hooda and others 2000). The rupture of domestic animal waste lagoons can cause multi-species fish kills in the receiving waters (Burkholder and others 2007). High levels of ammonia (NH_3) coupled with hypoxia/anoxia can cause the immediate death of multiple species of fishes (Burkholder and others 1997). During flushing flow events in the Mara River, fish kills downstream of hippo pools are likely due to a similar set of factors (Dutton and others 2018).

Greenhouse Gases

The concentrations of dissolved CH_4 reported here for high-HSI hippo pools are among the highest ever reported for open water bodies. The dissolved CH_4 concentrations in small, temporary ponds in the northeastern United States are among the highest reported for lentic waters (37 μmol L^{-1}) primarily due to high terrestrial carbon loading from leaves and shallow depths (Holgerson and Raymond 2016). The high-HSI hippo pools studied here had an average CH_4 concentration for surface and bottom water concentrations of 435 μmol L^{-1}. Large volumes of occluded gas bubbles were observed in the sediments, and ebullition was readily visible in some sites, presumably reflecting high rates of sediment CH_4 production. Methanogenesis is likely fostered by the constant loading of organic matter and inorganic nutrients through egestion and excretion of hippos, the limited availability of terminal electron acceptors for anaerobic respiration (for example, NO_3^-, SO_4^{2-}, Fe), and the high water temperatures.

Conclusions

The input of organic matter and nutrients by hippos strongly influences the biogeochemical processes and ecology of pools as well as downstream channels in the Mara River system. The degree of changes in concentrations of biogeochemical variables is determined by the combined effect of the number of hippos within the pool and its water residence time during intervals between flushing flows, as reflected by the HSI. High-HSI hippo pools quickly become depleted of dissolved oxygen in response to an overload of organic matter (Wolanski and Gereta 1999; Dutton and others 2018; Stears and others 2018), and accumulate potentially toxic levels of the products of heterotrophic metabolism. The episodic flushing of the pools by flow events resets pools back to their alternative oxic state.

Frequent shifts between these alternative states create heterogeneity in space and time within the riverine ecosystem. Hippo use of riverine pools was likely a strong yet spatially variable driver of aquatic biogeochemistry throughout sub-Saharan Africa before hippo populations were extirpated from much of their native range. This study details the mechanisms by which hippos can alter the biogeochemical processes within hippo pools and in downstream receiving waters, and it highlights the interaction of hippo numbers with water residence time as an important mediator of biogeochemical state.

These findings have important implications for tropical rivers with hippo populations where increasing water abstractions are reducing river baseflows (LVBC and WWF-ESARPO 2010; McClain 2013; McClain and others 2014; Stears and others 2018). To maintain good water quality in river systems with hippos, maintaining the natural flow regime, for example, by minimizing hydrologic alterations by storage dams and excessive water abstraction, should be considered more important than regulating the size of the hippo population.

Acknowledgements

We thank the Government of Kenya and the National Council for Science and Technology for authorizing this research (NCST/RRI/12/1/BS-011/25). The National Museums of Kenya provided assistance with permits and logistics. Support in the field was provided by Brian Heath and the Mara Conservancy. Paul Geemi, James Landefeld and Jordan Chancellor provided field assistance. Access to the hippo pools was facilitated by Tarquin and Lippa Wood, Amani Mara Camp, and the wardens of the Maasai Mara National Reserve, the Mara Conservancy and Naboisho Conservancy.

Funding

Funding was provided by US National Science Foundation Grants to DMP and EJR (NSF DEB 1354053, 1354062, and 1753727); a Grant from the National Geographic Society to DMP; Grants from the Yale Tropical Resources Institute, the Yale Institute for Biospheric Studies and the Yale MacMillan Center for International and Area

Studies to CLD; and a fellowship from the Robert and Patricia Switzer Foundation to ALS.

Compliance with Ethical Standards

Conflict of interest The authors declare that they have no conflict of interest.

REFERENCES

APHA. 2006. Standard methods for the examination of water & wastewater. Washington, DC: American Public Health Association.

Atkinson CL, Capps KA, Rugenski AT, Vanni MJ. 2016. Consumer-driven nutrient dynamics in freshwater ecosystems: from individuals to ecosystems. Biol Rev 92:2003–23.

Bartzke GS, Ogutu JO, Mukhopadhyay S, Mtui D, Dublin HT, Piepho H-P. 2018. Rainfall trends and variation in the Maasai Mara ecosystem and their implications for animal population and biodiversity dynamics. PLoS One 13:e0202814.

Bastviken D. 2009. Methane. In: Likens GE, Ed. Encyclopedia of inland waters. Oxford: Academic Press. p 783–805.

Burkholder J, Libra B, Weyer P, Heathcote S, Kolpin D, Thorne PS, Wichman M. 2007. Impacts of waste from concentrated animal feeding operations on water quality. Environ Health Perspect 115:308–12.

Burkholder JM, Mallin MA, Glasgow HB, Larsen LM, McIver MR, Shank GC, Deamer-Melia N, Briley DS, Springer J, Touchette BW, Hannon EK. 1997. Impacts to a coastal river and estuary from rupture of a large swine waste holding lagoon. J Environ Qual 26:1451–66.

Chew Shit F, Ho L, Ong Tan F, Wong Wai P, Ip Yuen K. 2005. The African Lungfish, *Protopterus dolloi*, detoxifies ammonia to urea during environmental ammonia exposure. Physiol Biochem Zool 78:31–9.

Conley DJ, Carstensen J, Vaquer-Sunyer R, Duarte CM. 2009. Ecosystem thresholds with hypoxia. Hydrobiologia 629:21–9.

Dawson J, Pillay D, Roberts PJ, Perissinotto R. 2016. Declines in benthic macroinvertebrate community metrics and microphytobenthic biomass in an estuarine lake following enrichment by hippo dung. Sci Rep 6:37359.

Dutton CL, Subalusky AL, Hamilton SK, Bayer EC, Njoroge L, Rosi EJ, Post DM. 2020. Data for: alternative biogeochemical states of river pools mediated by hippo use and flow variability. Mendeley Data.

Dutton CL, Subalusky AL, Hamilton SK, Rosi EJ, Post DM. 2018. Organic matter loading by hippopotami causes subsidy overload resulting in downstream hypoxia and fish kills. Nat Commun 9:1951.

Ehrenfeld JG. 2010. Ecosystem consequences of biological invasions. In: Futuyma DJ, Shafer HB, Simberloff D, Eds. Annual review of ecology, evolution, and systematics, Vol. 41. Palo Alto: Annual Reviews. p 59–80.

Ellis PS, Shabani AMH, Gentle BS, McKelvie ID. 2011. Field measurement of nitrate in marine and estuarine waters with a flow analysis system utilizing on-line zinc reduction. Talanta 84:98–103.

Eltschlager KK, Hawkins JW, Ehler WC, Baldassare F. 2001. Technical measures for the investigation and mitigation of fugitive methane hazards in areas of coal mining. Washington, DC: U.S. Department of the Interior.

Friedrich J, Janssen F, Aleynik D, Bange HW, Boltacheva N, Çagatay MN, Dale AW, Etiope G, Erdem Z, Geraga M, Gilli A, Gomoiu MT, Hall POJ, Hansson D, He Y, Holtappels M, Kirf MK, Kononets M, Konovalov S, Lichtschlag A, Livingstone DM, Marinaro G, Mazlumyan S, Naeher S, North RP, Papatheodorou G, Pfannkuche O, Prien R, Rehder G, Schubert CJ, Soltwedel T, Sommer S, Stahl H, Stanev EV, Teaca A, Tengberg A, Waldmann C, Wehrli B, Wenzhöfer F. 2014. Investigating hypoxia in aquatic environments: diverse approaches to addressing a complex phenomenon. Biogeosciences 11:1215–59.

GLOWS. 2007. Water quality baseline assessment report (WQBAR), Mara River Basin, Kenya-Tanzania. Miami: Global Water for Sustainability Program, Florida International University.

Golterman HL, Clymo RS. 1969. Methods for chemical analysis of fresh waters. Oxford: International Biological Programme by Blackwell Scientific.

Groffman PM, Baron JS, Blett T, Gold AJ, Goodman I, Gunderson LH, Levinson BM, Palmer MA, Paerl HW, Peterson GD, Poff NL, Rejeski DW, Reynolds JF, Turner MG, Weathers KC, Wiens J. 2006. Ecological thresholds: the key to successful environmental management or an important concept with no practical application? Ecosystems 9:1–13.

Hamilton SK, Ostrom NE. 2007. Measurement of the stable isotope ratio of dissolved N2 in 15 N tracer experiments. Limnol Oceanogr Methods 5:233–40.

Holgerson MA, Raymond PA. 2016. Large contribution to inland water CO_2 and CH_4 emissions from very small ponds. Nat Geosci 9:222.

Holm S. 1979. A simple sequentially rejective multiple test procedure. Scand J Stat 6:65–70.

Hooda PS, Edwards AC, Anderson HA, Miller A. 2000. A review of water quality concerns in livestock farming areas. Sci Total Environ 250:143–67.

Hooper DU, Chapin FS, Ewel JJ, Hector A, Inchausti P, Lavorel S, Lawton JH, Lodge DM, Loreau M, Naeem S, Schmid B, Setala H, Symstad AJ, Vandermeer J, Wardle DA. 2005. Effects of biodiversity on ecosystem functioning: a consensus of current knowledge. Ecol Monogr 75:3–35.

Hosomi M, Sudo R. 1986. Simultaneous determination of total nitrogen and total phosphorus in freshwater samples using persulfate digestion. Int J Environ Stud 27:267–75.

Jäntti H, Hietanen S. 2012. The effects of hypoxia on sediment nitrogen cycling in the Baltic Sea. Ambio 41:161–9.

Kanga EM, Ogutu JO, Olff H, Santema P. 2011. Population trend and distribution of the Vulnerable common hippopotamus Hippopotamus amphibius in the Mara Region of Kenya. Oryx 45:20–7.

Kanga EM, Ogutu JO, Piepho H-P, Olff H. 2013. Hippopotamus and livestock grazing: influences on riparian vegetation and facilitation of other herbivores in the Mara Region of Kenya. Landsc Ecol Eng 9:47–58.

Kilham P. 1982. The effect of hippopotamuses on potassium and phosphate ion concentrations in an African Lake. Am Midl Nat 108:202–5.

Kitchell JF, O'Neill RV, Webb D, Gallepp GW, Bartell SM, Koonce JF, Ausmus BS. 1979. Consumer regulation of nutrient cycling. BioScience 29:28–34.

Lewison RL, Oliver W, Subgroup ISHS. 2008. Hippopotamus amphibius. The IUCN Red List of Threatened Species 2008: e.T10103A3163790.

Loong AM, Tan JYL, Wong WP, Chew SF, Ip YK. 2007. Defense against environmental ammonia toxicity in the African lungfish, *Protopterus aethiopicus*: bimodal breathing, skin ammonia permeability and urea synthesis. Aquat Toxicol 85:76–86.

Lovley DR, Phillips EJP. 1987. Rapid assay for microbially reducible ferric iron in aquatic sediments. Appl Environ Microbiol 53:1536–40.

LVBC, Wwf-Esarpo. 2010. Assessing reserve flows for the Mara River, Kenya and Tanzania. Kisumu: Lake Victoria Basin Commission of the East African Community.

Masese FO, Abrantes KG, Gettel GM, Bouillon S, Irvine K, McClain ME. 2015. Are large herbivores vectors of terrestrial subsidies for riverine food webs? Ecosystems 18:686–706.

McCauley DJ, Dawson TE, Power ME, Finlay JC, Ogada M, Gower DB, Caylor K, Nyingi WD, Githaiga JM, Nyunja J, Joyce FH, Lewison RL, Brashares JS. 2015. Carbon stable isotopes suggest that hippopotamus-vectored nutrients subsidize aquatic consumers in an East African river. Ecosphere 6:1–11.

McCauley DJ, Graham SI, Dawson TE, Power ME, Ogada M, Nyingi WD, Githaiga JM, Nyunja J, Hughey LF, Brashares JS. 2018. Diverse effects of the common hippopotamus on plant communities and soil chemistry. Oecologia 188:821–35.

McClain ME. 2013. Balancing water resources development and environmental sustainability in Africa: a review of recent research findings and applications. Ambio 42:549–65.

McClain ME, Subalusky AL, Anderson EP, Dessu SB, Melesse AM, Ndomba PM, Mtamba JOD, Tamatamah RA, Mligo C. 2014. Comparing flow regime, channel hydraulics, and biological communities to infer flow–ecology relationships in the Mara River of Kenya and Tanzania. Hydrol Sci J 59:801–19.

McNeil BI, Sasse TP. 2016. Future ocean hypercapnia driven by anthropogenic amplification of the natural CO_2 cycle. Nature 529:383.

Mermillod-Blondin F, Rosenberg R. 2006. Ecosystem engineering: the impact of bioturbation on biogeochemical processes in marine and freshwater benthic habitats. Aquat Sci 68:434–42.

Mnaya B, Mtahiko MGG, Wolanski E. 2017. The Serengeti will die if Kenya dams the Mara River. Oryx 51:581–3.

Murphy J, Riley JP. 1962. A modified single solution method for the determination of phosphate in natural waters. Analytica Chimica Acta 27:31–6.

Mwanake RM, Gettel GM, Aho KS, Namwaya DW, Masese FO, Butterbach-Bahl K, Raymond PA. 2019. Land use, not stream order, controls N_2O concentration and flux in the Upper Mara River Basin, Kenya. J Geophys Res Biogeosci 124:3491–506.

Naiman RJ. 1988. Animal Influences on Ecosystem Dynamics. BioScience 38:750–2.

Naqvi SWA, Bange HW, Farias L, Monteiro PMS, Scranton MI, Zhang J. 2010. Marine hypoxia/anoxia as a source of CH_4 and N_2O. Biogeosciences 7:2159–90.

Osborn SG, Vengosh A, Warner NR, Jackson RB. 2011. Methane contamination of drinking water accompanying gas-well drilling and hydraulic fracturing. Proc Natl Acad Sci 108:8172–6.

R Core Team. 2018. R: a language and environment for statistical computing. Vienna: R Foundation for Statistical Computing.

Rabalais NN. 2002. Nitrogen in aquatic ecosystems. AMBIO: A Journal of the Human Environment 31: 102-112.

Randall DJ, Tsui TKN. 2002. Ammonia toxicity in fish. Mar Pollut Bull 45:17–23.

Schmitz OJ, Wilmers CC, Leroux SJ, Doughty CE, Atwood TB, Galetti M, Davies AB, Goetz SJ. 2018. Animals and the zoogeochemistry of the carbon cycle. Science 362:3213.

Sirota J, Baiser B, Gotelli NJ, Ellison AM. 2013. Organic-matter loading determines regime shifts and alternative states in an aquatic ecosystem. Proc Natl Acad Sci 110:7742–7.

Smith LL, Broderius SJ, USEPA. 1976. Effect of hydrogen sulfide on fish and invertebrates. Duluth, Minn.: U.S. Environmental Protection Agency, Office of Research and Development, Environmental Research Laboratory.

Stears K, McCauley DJ, Finlay JC, Mpemba J, Warrington IT, Mutayoba BM, Power ME, Dawson TE, Brashares JS. 2018. Effects of the hippopotamus on the chemistry and ecology of a changing watershed. Proc Natl Acad Sci 115:E5028.

Stommel C, Hofer H, East ML. 2016. The effect of reduced water availability in the great Ruaha River on the vulnerable common hippopotamus in the Ruaha National Park, Tanzania. PLoS One 11:e0157145.

Stookey LL. 1970. Ferrozine—a new spectrophotometric reagent for iron. Anal Chem 42:779–81.

Subalusky AL, Dutton CL, Njoroge L, Rosi EJ, Post DM. 2018. Organic matter and nutrient inputs from large wildlife influence ecosystem function in the Mara River, Africa. Ecology 99:2558–74.

Subalusky AL, Dutton CL, Rosi-Marshall EJ, Post DM. 2015. The hippopotamus conveyor belt: vectors of carbon and nutrients from terrestrial grasslands to aquatic systems in sub-Saharan Africa. Freshw Biol 60:512–25.

Subalusky AL, Post DM. 2018. Context dependency of animal resource subsidies. Biol Rev 94:517–38.

Testa JM, Kemp WM. 2012. Hypoxia-induced shifts in nitrogen and phosphorus cycling in Chesapeake Bay. Limnol Oceanogr 57:835–50.

Vanni MJ. 2002. Nutrient cycling by animals in freshwater ecosystems. Annu Rev Ecol Syst 33:341–70.

Wolanski E, Gereta E. 1999. Oxygen cycle in a hippo pool, Serengeti National Park, Tanzania. Afr J Ecol 37:419–23.

Zar J. 2010. Biostatistical analysis, Vol. 1. 5th edn. Upper Saddle River: Prentice Hall. pp 389–94.